
Modelling the Sea Level of the Upper Bay of Fundy

Frédéric Dupont, Charles G. Hannah and David Greenberg

Fisheries and Oceans Canada, Bedford Institute of Oceanography

P.O. Box 1006, Dartmouth NS B2Y 4A2

[Original manuscript received 30 December 2003, in revised form 3 August 2004]

ABSTRACT A high resolution model of the upper Bay of Fundy was developed to simulate the tides and sea level. The model includes the wetting and drying (inundation) of the extensive tidal flats in Minas Basin. The model reproduces the dominant M_2 tidal harmonic with an error on the order of 0.30 m, and the total water level in Minas Basin with an r.m.s. error of 0.30–0.50 m. Overall the system is capable of a sea level simulation with a relative error of ~10%. The motivation for the model development was the simulation of the land/water interface (instantaneous coastline) to aid in the validation of coastline retrieval algorithms from remotely sensed observations. Comparison of observed and simulated coastlines showed that a high quality representation of the local topography/bathymetry is as important as the sea level simulation in the calculation of the coastline. For example, long narrow features such as dykes are difficult to resolve in a dynamical model but are important for the inundation of low lying areas.

RESUMÉ [Traduit par la rédaction] Un modèle à haute résolution du fond de la baie de Fundy a été mis au point pour simuler les marées et le niveau de la mer. Le modèle tient compte du mouillage et du séchage (inondation) des vastes bas fonds intertidaux du bassin des Mines. Le modèle reproduit l'harmonique dominante de la marée M_2 avec une erreur de l'ordre de 0,30 m et le niveau d'eau total dans le bassin des Mines avec une erreur quadratique de 0,30 - 0,50 m. Dans l'ensemble, le système est capable de simuler le niveau de la mer avec une erreur relative de ~10 %. Ce modèle a été mis au point pour simuler l'interface terre/eau (la ligne de côte instantanée) dans le but d'aider à valider les algorithmes d'extraction des lignes de côte à partir d'observations de capteurs à distance. La comparaison des lignes de côte observées et simulées montre qu'une représentation de haute qualité de la topographie/bathymétrie locale est aussi importante que la simulation du niveau de la mer dans le calcul de la ligne de côte. Par exemple, les caractéristiques longues et étroites, comme les digues, sont difficile à résoudre dans un modèle dynamique mais sont importantes du point de vue de l'inondation des régions basses.

1 Introduction

This paper reports on the development of a sea level prediction system for the upper Bay of Fundy (Fig. 1). The motivation is the simulation of the land-water boundary (instantaneous coastline) in the Bay as part of the validation of the land-water boundary derived from remotely sensed observations (e.g., RADARSAT-1, polarimetric Synthetic Aperture Radar (SAR), Compact Airborne Spectrographic Imager (CASI), Landsat and Ikonos imagery) as described by Deneau (2002) and Milne (2003). This application has two requirements beyond accurate simulation of the sea level: a wetting and drying capability, since the coastline needs to be predicted by the model; and accurate local bathymetry/topography in the area for the comparisons, since small changes in height/depth can lead to large changes in the modelled coastline. The focal region here is Minas Basin, in particular the area around Wolfville, NS.

The dominant feature of the sea level variability in the Bay of Fundy is the M_2 tide which varies in amplitude from 3 m at Saint John to over 6 m at the head of the Minas Basin. The reason for the large tides is the fact that the natural frequency

of oscillation in the Gulf of Maine and the Bay of Fundy system is close to that of the M_2 tide (Garrett, 1972, 1974). While the M_2 tide dominates the sea level variability, other tidal constituents must be modelled in order to achieve the target accuracy of 0.3–0.5 m in Minas Basin. The N_2 and S_2 constituents have amplitudes on the order of 1 m and other semi-diurnal constituents have amplitudes on the order of 0.1 m. In addition, remotely generated sea level disturbances that propagate into the Bay can contribute greatly to the variability.

The M_2 tide in the Gulf of Maine and the Bay of Fundy system was modelled successfully by Greenberg (1979) using a series of four nested meshes with resolutions ranging from 21 km in the Gulf of Maine to 1.6 km in Minas Basin. An accuracy of 0.15 m and 5° in phase was generally achieved in the Bay of Fundy with the exception of Minas Basin where the phases were greater than observed and the amplitudes were too large. The model was extended by DeWolfe (1986) to include other constituents (N_2 , S_2 , O_1 , K_1) but the work focused on the potential impacts of tidal power development

*Corresponding author's e-mail: hannahc@mar.dfo-mpo.gc.ca

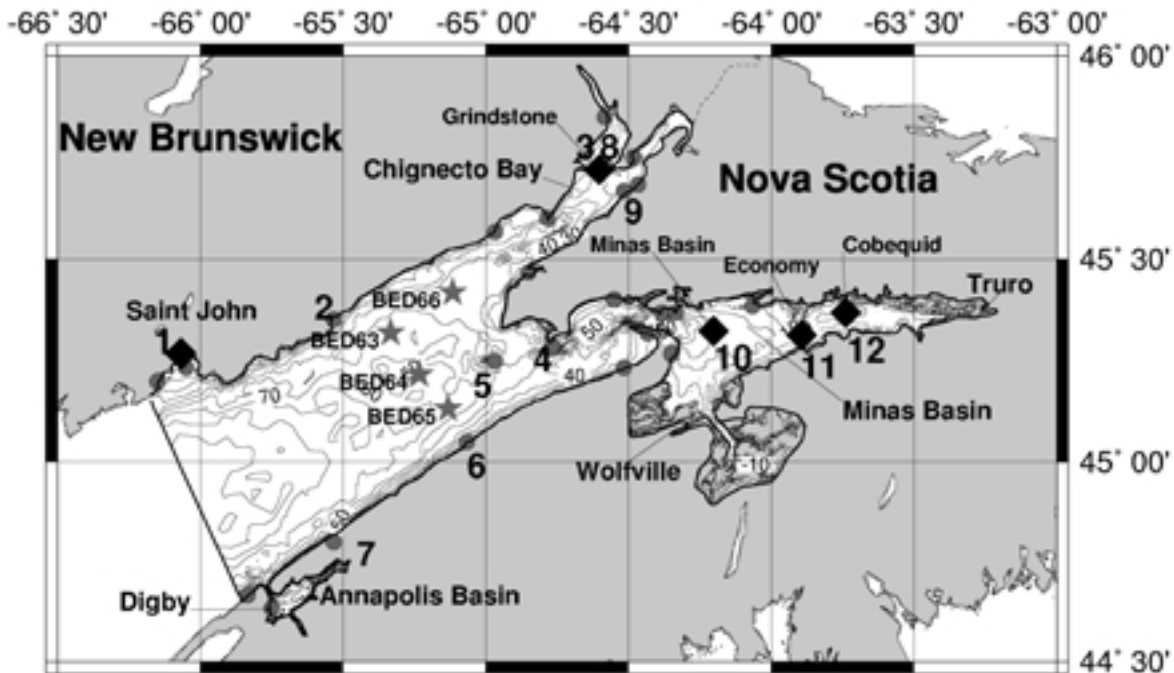


Fig. 1 Map of the upper Bay of Fundy showing the locations of the tide gauge stations (grey circles) and the time series stations (black diamonds). Velocity stations are labelled with a grey star. The bathymetry is contoured with thin black lines and the computational domain boundary is shown in thicker black lines. Areas below mean sea level are white and areas above mean sea level are grey. Minas Channel is the narrow channel that connects Minas Basin to the rest of the Bay of Fundy.

and a detailed comparison with observations was not reported. Recently, Sankaranarayanan and McCay (2003) modelled five tidal constituents (M_2 , N_2 , S_2 , O_1 , K_1) in the Bay of Fundy in support of work in Saint John harbour and achieved errors of less than 0.2 m in amplitude and 7° in phase for M_2 , with the exception of Minas Basin where the errors increased to 0.3–0.5 m (relative to an amplitude of 4.5–6 m). The errors in N_2 (the next largest component) were 0.1–0.3 m in Minas Basin (relative to an amplitude of 0.7–1 m) with phase errors as large as 20° (roughly a 40-minute error in timing). Their model resolution ranged from 50–100 m in Saint John Harbour to 2–3 km in the Bay of Fundy.

In this paper we develop a sea level prediction system for the upper Bay of Fundy. The system includes multiple tidal constituents (M_2 , N_2 , S_2 , O_1 , K_1 , plus the four minor semidiurnal constituents K_2 , L_2 , $2N_2$, ν_2) and uses the Saint John tide gauge record to provide corrections to the open boundary forcing when hindcasting the instantaneous coastline. The system is based on the finite element method so that high resolution can be added where it is required. The model includes wetting and drying of tidal flats allowing for simulation of the instantaneous coastline.

The paper is composed as follows. The components of the prediction system are described in Section 2 and the model validation is presented in Section 3. In Section 4 we compare the simulated and observed instantaneous coastline for two cases and Section 5 provides an error assessment of the three major semidiurnal tidal constituents. Section 6 contains a discussion of the results with a focus on issues that will need to

be addressed to reduce the model errors. Conclusions are given in Section 7.

2 The modelling system

a The Model

The model, *Modèle aux Ondes de Gravité – 2 Dimensions (MOG-2D)* (Carrère and Lyard, 2003), is a two-dimensional model that uses the finite element method to solve the shallow water equations that describe the dynamics of the depth averaged oceanic flow. The model, written by Dave Greenberg, Bedford Institute of Oceanography (BIO) and Florent Lyard, Laboratoire d'études en géophysique et océanographie spatiales – Centre national de recherches scientifique (LEGOS-CNRS), is based on the generalized wave equation (Lynch and Werner, 1991; Lynch et al., 1996) using spherical coordinates (Greenberg et al., 1998). It was used successfully by Dupont et al. (2002) to model the tides in the north-west Atlantic, including the Bay of Fundy.

The wetting and drying of tidal flats was incorporated following the methodology of Greenberg et al. (2005). As the water level falls and the elevation at one node of an element falls under the sea bottom, the nodal velocity is set to zero, but the elevation remains active and is free to move. If the elevations at all three vertices of an element fall under the sea bottom, this element is considered dry and is counted as an island (or part of one) and not used in the construction of the wave equation matrix (i.e., we have created a hole in the mesh). When a node falls strictly inside such an island, it is deemed

inactive and its elevation is frozen. A rising water level will raise the elevation at all active nodes, including those along the perimeter of islands. When the elevation at one vertex of a dry element rises above the sea bottom, this element is no longer considered dry and all of its elevation points are unfrozen. This process can continue until the entire island has been removed. Beaches, or dry areas connected to lateral boundaries, are handled in the same way. Once the elevation at all nodes is above the sea bottom, the water is constrained only by the lateral boundaries of the mesh.

The model uses a quadratic drag law for dissipation and we use the standard drag coefficient for vertically averaged tidal models, $C_d = 2.5 \times 10^{-3}$. Horizontal mixing is parametrized using the Smagorinsky (1963) formulation as implemented by Lynch et al. (1996).

b *The Mesh*

The model domain covers the upper Bay of Fundy and includes potentially inundated areas with a maximum elevation above mean sea level of 20 m (Fig. 1). Three areas, the Annapolis Basin, and the vicinity of Wolfville and of Truro, were specifically targeted.

The ocean and land topography were obtained from several sources at differing resolution and coverage. The initial ocean data were obtained from a digital version of Canadian Hydrographic Service (CHS) chart 4010 – Bay of Fundy (Inner Portion). These were augmented with high resolution multibeam data in limited areas of Minas Channel and Chignecto Bay. The land topography for the nearshore was obtained from Tim Webster and Robert Maher of the Applied Geomatics Research Group (Centre of Geographic Sciences, Middleton NS, Canada) and included data from digital versions of land based topographic charts and high density LIDAR data covering the land and some intertidal areas in the Annapolis Basin, and in the vicinity of Wolfville and Truro. Because of the volume of topographic data, it was thinned to roughly 30-m resolution to balance acceptable resolution with computational resources. The final dataset used close to Wolfville, NS is shown as an example in Fig. 2.

The final number of nodes in the mesh is close to 75000 with resolution between 30 m and 5 km (Fig. 3). The time integration is explicit with a timestep of 2 s. An M_2 tidal cycle can be computed in three hours and 30 minutes on a 1600 Mhz PC (about 3.5 days simulated in one day).

c *Tidal Boundary Conditions*

The open boundary runs approximately along a straight line from Digby to Saint John (Fig. 1). The tidal open boundary conditions for the elevation were obtained from the solution of a regional assimilation system following the procedure described in Dupont et al. (2002) and using satellite altimetry data only (harmonic analysis for the tidal constituents at the cross-over points of the TOPEX/Poseidon data). The domain for this assimilation system is shown in Fig. 4 and covers the Gulf of Maine, the Bay of Fundy and part of the Scotian Shelf. The system assimilated tidal harmonic data at twelve

TOPEX/Poseidon crossover points for nine tidal constituents (M_2 , N_2 , S_2 , K_1 , O_1 , K_2 , L_2 , $2N_2$, v_2). The harmonic constituents were then interpolated along the open boundary of the high resolution model of the upper Bay of Fundy.

The regional assimilation system uses the observations, in this case the tidal harmonics at the TOPEX/Poseidon crossover points (Fig. 4), to compute tidal boundary conditions at the boundary of the regional mesh. The procedure involves running a forward model which transforms specified boundary conditions into tidal harmonics at the observation locations and an inverse model which transforms the differences between the modelled and observed tidal harmonics into changes in the specified boundary conditions. The forward model is MOG-2D. The inverse model is the linear harmonic model TRUXTON (Lynch et al., 1998) modified to use spherical polar coordinates and to accept a two-dimensional field of root-mean-square (r.m.s.) velocity from the forward model for computing a spatially variable drag coefficient. The multi-constituent tidal boundary conditions are computed in an iterative fashion involving multiple runs of the forward and inverse models. Each iteration required nine solutions with the inverse model (one for each constituent) and a 240-day run with the forward model in order to resolve the different constituents in the tidal analysis. The details of the procedure and the smoothing parameters are given in Dupont et al. (2002).

The choice of constituents was based largely on Table 1 which shows the fifteen largest tidal constituents in the Bay of Fundy. Our nine constituents include eight of the top ten. At Saint John, the nine constituents represent 88% of the sum of the amplitudes of the 67 official tidal constituents (we exclude the chart datum Z0). The constituents μ_2 and λ_2 were excluded because they proved difficult to assimilate in our regional model. The likely reason is errors in the harmonic analysis of the TOPEX/Poseidon data for these constituents because their frequencies are too close to the preceding constituents. The M_4 constituent was also excluded as the results did not compare well with the observed constituents at Boston and Saint John.

d *Hindcasting the Total Water Level*

For hindcasting the water level for a particular period we used the tidal boundary conditions plus a sea level correction based on the hourly sea level at Saint John, the only permanent tide gauge in the Bay of Fundy. No wind forcing or air pressure corrections were used.

The first step in the correction process was to compute a prior estimate of the time series of modelled sea level at Saint John. This was computed in two different ways. The first one (Correction 1) consisted of predicting the elevation at Saint John based on the harmonic constituents of the regional assimilation system. The second method (Correction 2) required an initial run of the high resolution model with the open boundary forcing based on the constituents from the regional assimilation system.

For each method, the correction time series was the difference between the observed and simulated elevation at Saint

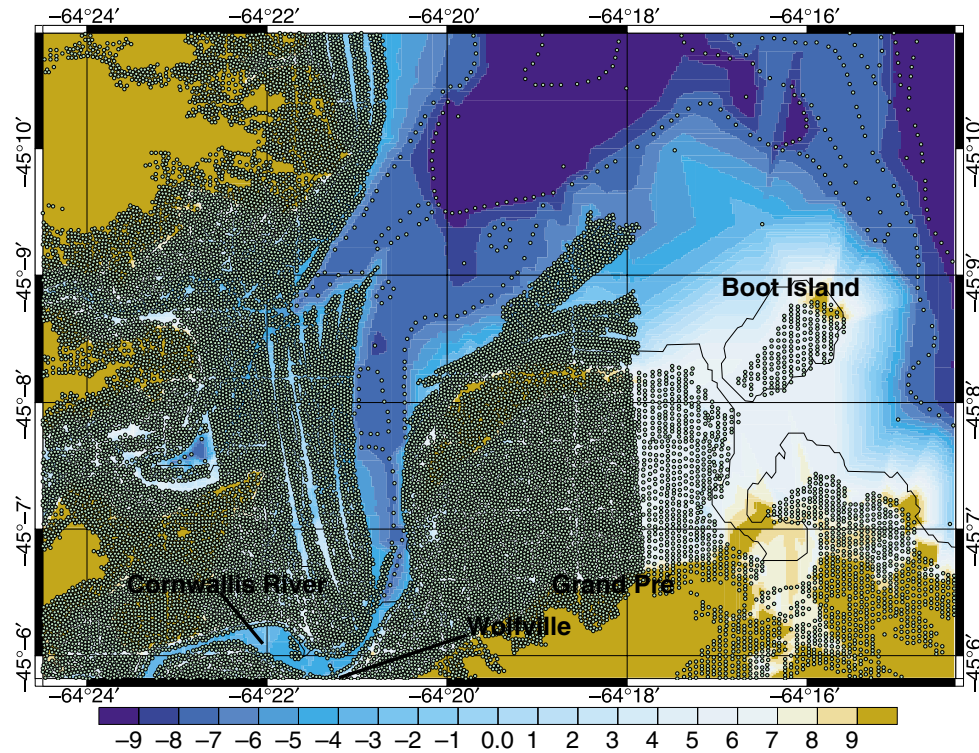


Fig. 2 Locations of the high resolution bathymetry data (green circles) used in reconstructing the model depth, close to Wolfville, NS. The thin black contour line is an approximate coastline used for plotting purposes. The colour represents the bathymetry/topography field interpolated from the dataset (positive is above mean sea level). The units are metres.

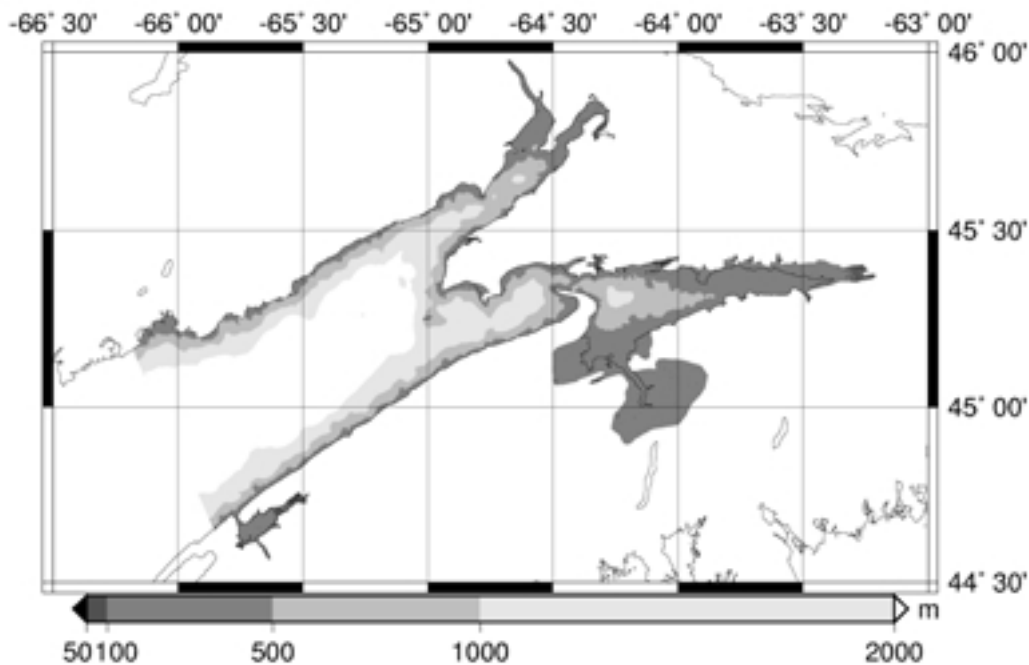


Fig. 3 Local mesh resolution (m) shown in grey scale.

John for the time period of interest. For hindcasting, the model was run with the nine tidal constituents plus the hourly correction time series. The correction was applied uniformly along the boundary.

The correction is needed because of unresolved processes affecting sea level such as storm surge, other tidal constituents, baroclinicity or simply because of modelling errors. In the hindcasts, the remaining discrepancy between the

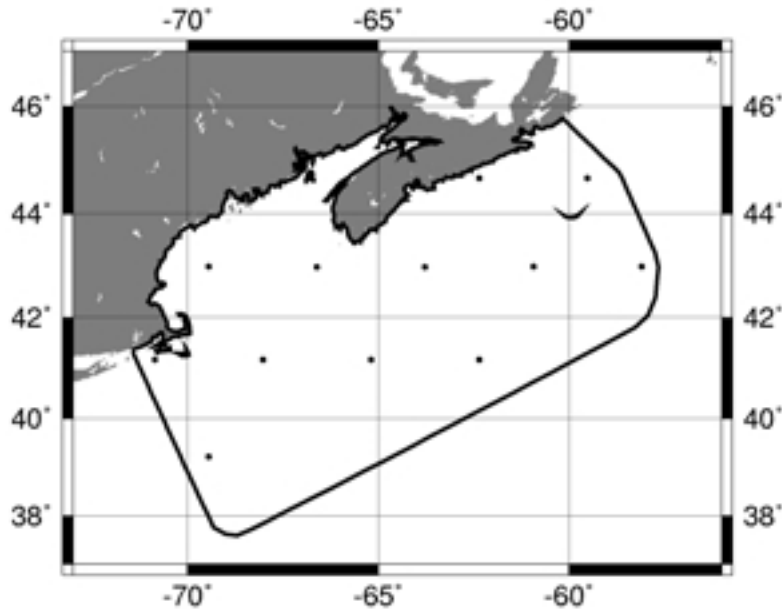


Fig. 4 The computational domain used in the assimilation scheme for deriving the tidal boundary conditions for the Bay of Fundy model. The solid dots are the TOPEX/Poseidon cross-over points where the tidal harmonics were specified from the analysis of the satellite altimetry.

TABLE 1. Mean observed amplitude for the different tidal constituents in the Bay of Fundy. The third column (N) is the number of stations that report that constituent.

	Ampl. (m)	N
M_2	4.27	36
N_2	0.863	36
S_2	0.646	36
L_2	0.396	16
K_2	0.177	33
ν_2	0.172	10
K_1	0.171	36
μ_2	0.123	15
O_1	0.122	36
λ_2	0.095	7
M_4	0.083	36
$2N_2$	0.079	9
OP_2	0.067	5
MKS_2	0.066	7
M_6	0.064	18

simulated and observed elevation at Saint John was generally small, however, the model-data discrepancy did increase away from Saint John.

3 Validation

a The Tides

The tidal validation simulation was carried out using the five major constituents (M_2 , N_2 , S_2 , K_1 , O_1) run simultaneously. Table 2 shows the validation for the M_2 constituent at the 12 stations common to Greenberg (1979)¹ and Sankaranarayanan and McCay (2003). Overall the amplitude and phase errors are quite small with a mean amplitude error of 0.12 m and a

mean phase error of 2.4° . The model under-predicts the amplitude by about 0.2 m in Minas Basin and over-predicts the phase by only a few degrees.

The error metric in the last column of Table 2 is the distance in the complex plane between the observed and modelled constituents

$$E = \left| A_o e^{i\phi_o} - A_m e^{i\phi_m} \right| \quad (1)$$

where A_o , ϕ_o are the amplitude and phase of the observed harmonic and A_m , ϕ_m are the amplitude and phase of the modelled harmonic. This error metric, which combines the amplitude and phase errors into a single quantity, will be used as the primary metric for this validation. As an overall error for a single constituent we will use the r.m.s. value computed over all the stations (0.26 m for the stations in Table 2). We note that the 2.6° phase error (about 5 min) makes a larger contribution to the overall error than the 0.14 m amplitude error.

The new high resolution model has smaller M_2 errors than previous models. Using the error metric, Eq. (1), the r.m.s. error in this model is 0.26 m compared with 0.36 m for Greenberg (1979) and 0.45 m for Sankaranarayanan and McCay (2003). Note that the present model has not been tuned to fit any coastal data, whereas the Greenberg model was carefully tuned for bottom friction and some bathymetric features, and the model of Sankaranarayanan and McCay (2003) was tuned to fit the elevation record at Saint John.

The validation data for all five constituents against the 29 stations in the Bay of Fundy (Fig. 1) is shown in the polar plots in

¹with additional information extracted from Table 4.1 of Bay of Fundy Tidal Power Review Board (1977)

TABLE 2. Observed and modelled amplitude (m) and phase (degrees GMT), and discrepancies (Obs.-Model) for M_2 . The ‘Error’ in the last column is the error metric described in the text. The stations are those common among Greenberg (1979) and Sankaranarayanan and McCay (2003). The second column is the key to the station numbers in Fig. 1.

Stations	#	Observed		Modelled		Differences		Error (m)
		Ampl.	phase	Ampl.	phase	Ampl.	phase	
Saint John	1	3.04	98.2	3.00	98.6	0.04	-0.3	0.04
St. Martins	2	3.69	101.6	3.64	103.4	0.04	-1.8	0.12
Grindstone Isl.	3	4.72	107.0	4.60	108.1	0.11	-1.0	0.14
Cape d’Or	4	4.34	102.0	4.27	106.0	0.07	-4.0	0.31
Ile Haute	5	4.15	99.2	4.04	101.8	0.11	-2.5	0.21
Margaretsville	6	3.86	92.9	3.85	96.5	0.01	-3.6	0.24
Parkers Cove	7	3.43	89.8	3.28	91.3	0.16	-1.5	0.18
Grindstone	8	4.86	104.4	4.61	108.0	0.25	-3.6	0.39
Cumberland Basin	9	4.74	104.6	4.63	107.2	0.11	-2.6	0.24
Minas Basin	10	5.54	120.8	5.33	122.6	0.20	-1.7	0.26
Economy	11	5.92	125.4	5.71	128.2	0.22	-2.8	0.35
Cobequid Bay	12	6.12	129.3	5.94	132.8	0.18	-3.5	0.41
Mean		4.53	-	4.41	-	0.12	-2.4	0.24
r.m.s.		4.63	-	4.50	-	0.14	2.6	0.26

Fig. 5. Overall, the simulated M_2 and N_2 components have a bias towards small amplitudes and late phases. The M_2 amplitude errors are generally 0.1–0.2 m and the phase errors are late by 1–3°. The N_2 amplitude errors are generally small (< 0.05 m) but at six stations they exceed 0.1 m, and the phases are late by 10–15°. The S_2 component has a weak bias towards positive amplitude errors and a bias towards late phases. The amplitude errors are generally small (~0.05 m) with large errors at a few sites. The S_2 phase errors are also small, generally ~5°, with errors as large as 16° at a few sites. The O_1 and K_1 amplitude and phase errors are typically small, less than 0.03 m and 10°, and with no obvious pattern.

The overall quantitative comparison against the same data is shown in Table 3. For M_2 the agreement is much better than previously obtained by Dupont et al. (2002); 0.28 m instead of 0.77 m. The improvement likely comes from the improved resolution of the bathymetry. On the other hand, the accuracy of N_2 degraded (0.26 m instead of 0.19 m). Compared to the regional assimilation system, there is some improvement in M_2 when a higher resolution is used although we again note the poorer agreement for N_2 . For S_2 , K_1 and O_1 the error levels are about the same among the three modelling systems.

To estimate the confidence limits on the observed tidal harmonics, an error analysis was performed using the Minas Basin time series (89 days of data in the spring of 1976; see DeWolfe (1977)). The tidal and error analysis was carried out using T_TIDE (Pawlowicz et al., 2002) and its linear error analysis. For the full 89-day record, the 95% confidence limit on the amplitudes of the semidiurnal constituents was 0.07 m and the confidence limits on the phase were 1°, 4° and 9° for M_2 , N_2 and S_2 , respectively. Confidence limits computed using the non-linear bootstrap method were sensitive to the choice of error model and were generally larger than the linear estimates. Similar results were obtained for the other data from the spring of 1976 (from DeWolfe (1977)). The 95% confidence limits on 29-day intervals were two to three times larger. In the Bay of Fundy tidal database, nine of the records are 29 days long or less and only four are longer than 90 days.

TABLE 3. The r.m.s. elevation error (m) based on the error metric Eq. (1) for each tidal constituent for 29 stations in the Bay of Fundy. Stations for which the model solution exhibited wetting/drying were excluded from the comparison. The first line corresponds to the present high resolution model, the second to the regional assimilation system and the third to Dupont et al. (2002).

Model	M_2	N_2	S_2	K_1	O_1
present	0.28	0.26	0.12	0.03	0.02
regional	0.32	0.21	0.12	0.02	0.02
NW Atl.	0.77	0.19	0.15	0.03	0.02

All of the records listed in Table 2 are longer than 29 days and most are longer than 80 days. Adopting the 95% confidence limits for the 89-day analysis, we see that for M_2 the bias in amplitude and phase is outside the 95% confidence limits (0.07 m, 1°). In particular, the three stations in Minas Basin (Minas Basin, Economy and Cobequid) have amplitude errors about three times the limit. For N_2 the amplitude errors at most stations are less than 0.07 m, however, the phase errors are generally larger than the confidence limit of 4°. For S_2 the amplitude and phase errors are within the 95% confidence limits at most stations. We will analyse the M_2 and N_2 errors further in Section 5.

The model velocities were compared with analysed constituents from the four locations in the Northwest Atlantic Tidal current database (Drozdowski et al., 2002) that were inside our computational domain (Fig. 1). None were found in Minas Basin. For M_2 , the maximum observed velocity is around 1 m s⁻¹. Qualitatively, the agreement is excellent for all three semidiurnal constituents (Fig. 6). The agreement is also good (although slightly poorer) for the diurnal constituents except at station BED66. For quantitative comparisons, we define a velocity error metric for each constituent as the r.m.s. of the distance between two points turning simultaneously around the observation and model tidal ellipses, respectively (Table 4). This error metric is particularly sensitive to phase errors, which are the primary culprits when the

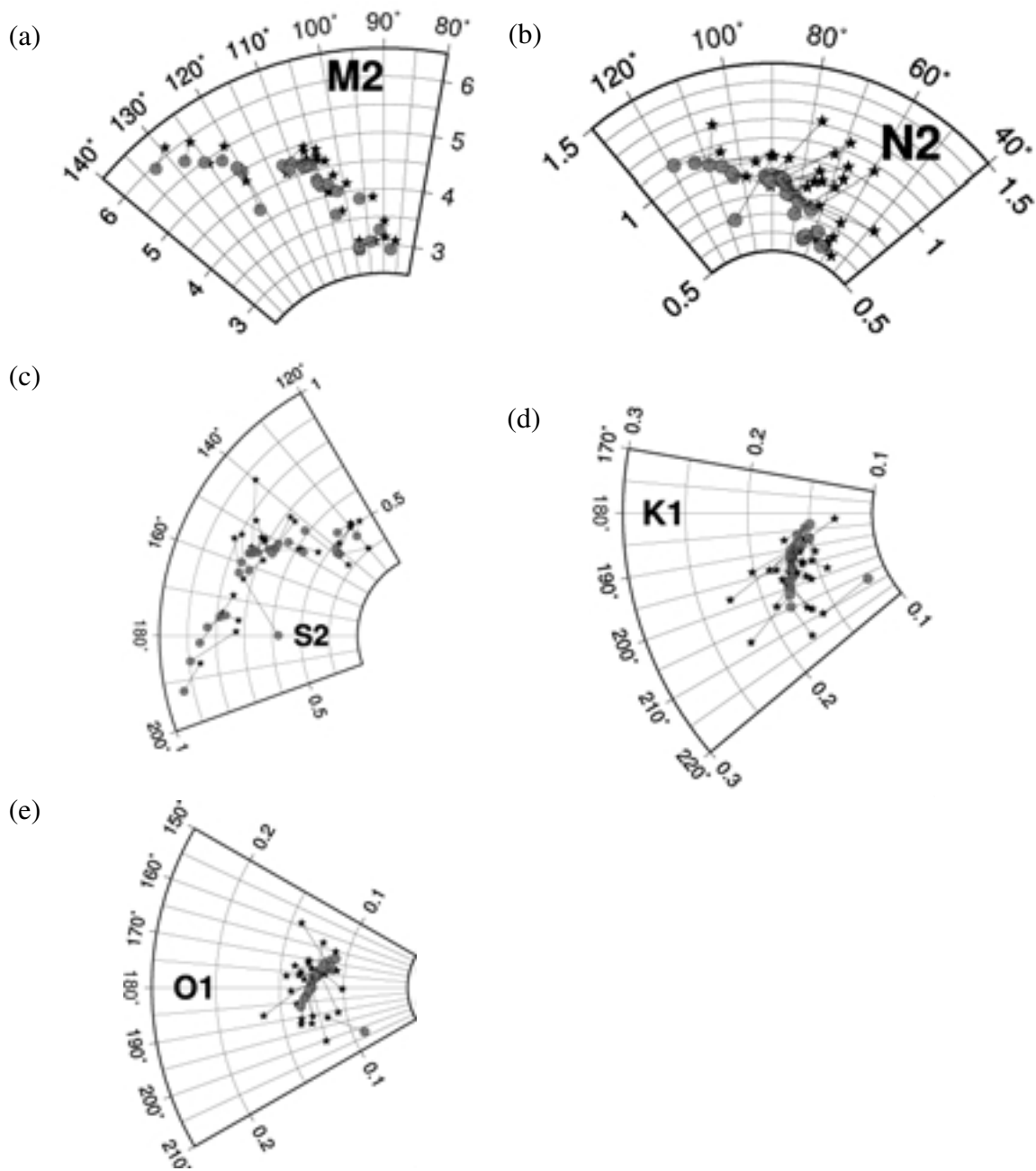


Fig. 5 Polar plot of the model (grey solid circles) versus observations (black stars) for the five major constituents.

qualitative agreement is good but the error metric is large. Since velocity errors are commonly larger than elevation errors, a 20% error would be considered a good match. The largest error found is 12% for M_2 , 16% for N_2 and S_2 , 22% for O_1 and 28% for K_1 . The error is therefore in the acceptable range for M_2 and the other semidiurnal constituents but poor for the diurnal constituents. The high quality of the N_2 tidal currents was a surprise given the errors in the N_2 elevations. The error in N_2 at the station closest to the current meters (Ile Haute, Station 5 in Fig. 1) was -0.03 m for ampli-

tude and 19° for phase. The good agreement with the velocities may indicate that the quality of the N_2 analysis at some of the tide gauges is weak.

Given the encouraging agreement with the tidal velocities it is of interest to look at the spatial patterns of the energy dissipation by bottom friction. The dissipation by bottom friction is defined here as $\rho C_d \langle |u|^3 \rangle$ where, $\rho = 1025 \text{ kg m}^{-3}$ is a standard value for sea water density and C_d is the drag coefficient. We computed mean values of $\langle |u|^3 \rangle$ from a 32-day run (the 1976 May hindcast-period) with the nine-constituent model.

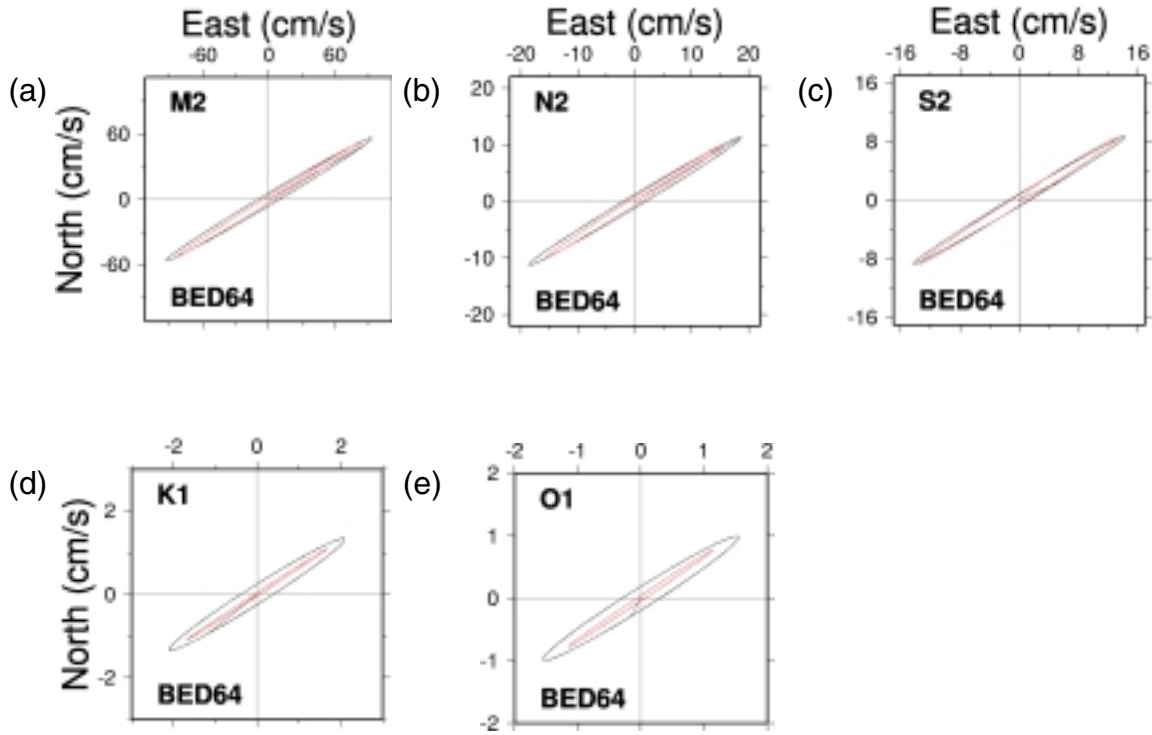


Fig. 6 Observed and modelled tidal ellipses. The dark ellipses are the depth-averaged observations and the red ones are the model estimate at the same location. Units are cm s^{-1} .

TABLE 4. The tidal velocity errors at four locations in the Bay of Fundy. The error metric for each constituent is the r.m.s. of the distance (in cm s^{-1}) between two points turning simultaneously around the observed and modelled tidal ellipses, respectively. The first metric is the absolute error in cm s^{-1} and the second is the error relative to the major axis of the observed tidal ellipse.

	M_2 error		N_2 error		S_2 error		K_1 error		O_1 error	
	cm s^{-1}	%								
BED63	4.62	5.17	1.82	10.1	1.02	7.4	0.438	22	0.185	13.6
BED64	9.01	8.29	3.12	14.3	1.59	9.51	0.691	27.8	0.4	21.8
BED65	12	11.5	3.39	16.2	2.57	15.9	0.136	6.28	0.196	11.8
BED66	7.85	10.8	1.72	11.9	1.82	16.5	0.579	28.6	0.421	28.3

In the Minas Basin area, an arc of very high values occupies Minas Channel at about 50 to 60 W m^{-2} where currents in the bay are the strongest (Fig. 7). Greenberg (1979), looking at M_2 only, found a dissipation of about 100 W m^{-2} at about the same location². A band of high values (1 – 10 W m^{-2}) extends to the east, down the main channel. At the eastern end of Minas Basin, one bank stands out with values just above 10 W m^{-2} .

In the intertidal areas (regions defined as shallower than 6 m), velocities are much less than along the main channel and local dissipation rates are much lower. There are, however, thin bands of values between 0.2 to 1 W m^{-2} located in three river beds in the Wolfville vicinity and along or close to the extreme position of high tides.

b The Total Water Level

For validation of the total water level, the nine tidal constituents plus the correction derived from the Saint John tide gauge were used. The model predictions were compared with hourly records from the Saint John tide gauge and four sub-surface pressure gauges deployed during May 1976 (DeWolfe, 1977): three in Minas Basin (Minas, Economy and Cobequid) and one in Chignecto Bay (Grindstone). Table 5 shows the r.m.s. error of the hourly time series at the five stations. Without any correction, the error ranges from 0.2 m at Saint John to 0.6 m at the head of Minas Basin (Cobequid). Correction 1 reduces the error by 0.05 – 0.08 m . Correction 2 reduces the error by a further 0.03 to 0.1 m , with the largest

²As our main goal was to look at the spatial patterns of the dissipation, we have not investigated the reasons for the discrepancy between the models. Nonetheless, both models have similar broad structures. We report here on the smaller scale structures found in our model.

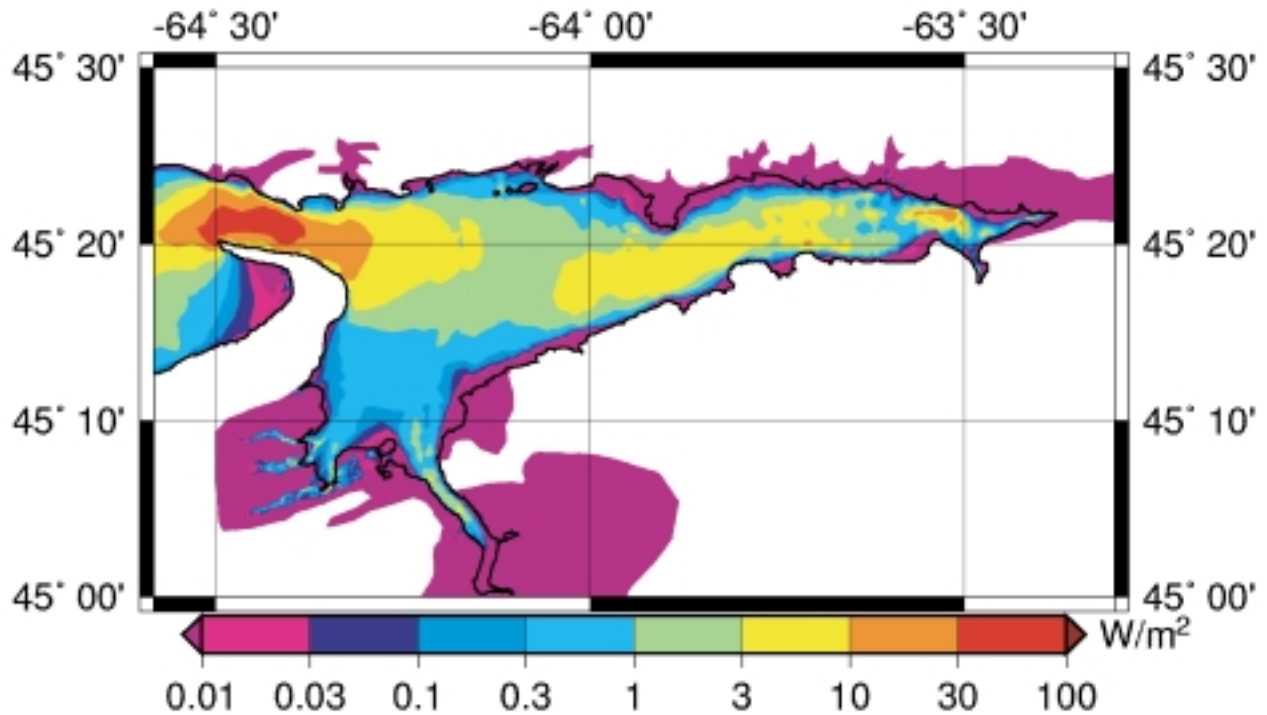


Fig. 7 Frictional dissipation ($W\ m^{-2}$) in Minas Basin. The thicker black line is the coastline based on mean sea level.

TABLE 5. The r.m.s. timeseries elevation error (m) at five locations using no correction and the two correction methods. The mean values were removed prior to the analysis so that all elevations are relative to mean sea level. The period for comparison was 1 May to 4 June 1976.

Correction	Saint John	Minas	Grindstone	Economy	Cobequid
None	0.20	0.42	0.47	0.51	0.58
Corr.1	0.13	0.36	0.41	0.44	0.53
Corr.2	0.03	0.27	0.37	0.38	0.50

improvement occurring at Saint John. Hereafter, Correction 1, which does not require running the model twice, will be used. We return to the question of the error in Section 5.

4 Predicting the land/water interface in Minas Basin

An automatic procedure was designed to produce elevation fields (based on Correction 1) at the exact date and time of the remotely sensed images. Seven snapshots were provided for analysis and comparison with the coastlines derived from the images as reported by Milne (2003). Here we provide a qualitative interpretation of two snapshots that illustrate the strengths and weaknesses of the simulations.

Filling the gaps in the Saint John sea level data needed for the correction procedure was an important issue. For example, in the five-day period leading up to the 13 September 1999 snapshot (Fig. 8) about 14% of the data were missing and for 13 July 2000 (Fig. 9) all of the data were missing. Data gaps were filled by a time-series reconstructed from the

TABLE 6. The r.m.s. elevation error (m), computed as in Table 3, for different values of the bottom friction coefficient (C_d) and using the corrected M_2 at the open boundary. The value $C_d = 2.5 \times 10^{-3}$ is the base case.

C_d	M_2	N_2	S_2	K_1	O_1
2.5×10^{-3}	0.24	0.23	0.12	0.03	0.02
2.0×10^{-3}	0.25	0.21	0.11	0.02	0.02
1.5×10^{-3}	0.40	0.19	0.11	0.03	0.03

official tidal constituents at Saint John. For the periods considered, the r.m.s. difference between the reconstructed time-series and the actual observations (i.e., the nontidal component) varied between 0.10 and 0.22 m. For comparison, the r.m.s. difference between the observed and modelled (with Correction 1) Saint John elevation varied between 0.11 and 0.20 m. Thus the uncertainties associated with missing data are of the same order as the hindcasting errors at Saint John and less than the hindcasting errors in Minas Basin (0.3–0.5 m).

In the automatic procedure, the model is spun up from rest five days prior to the date of interest. The model tidal forcing is ramped up for the first 12 hours from zero to full and is fixed at full forcing for the duration of the simulation. The model stops at the desired date and time and outputs the elevation field. From this elevation field, the model coastline is defined as the set of points where the water surface meets the bottom.

The procedure for deriving coastlines from remotely sensed observations can be found in Deneau (2002) and Milne (2003).



Fig. 8 True colour Landsat-7 image of the Wolfville vicinity at 14:54:13 (GMT) on 13 September 1999. The image was taken near low tide. The green is vegetation and the sandy brown is exposed tidal flats. The red line is the instantaneous coastline extracted from one of the near infra-red bands and the blue line is the coastline extracted from the tidal model. The analysis is reported in Milne (2003). Image courtesy of Trevor Milne and the Applied Geomatics Research Group.

For Landsat images the procedure uses the optical properties of water in the infra-red spectral range. In this spectral range, water appears very dark and can be clearly separated from land features. After some filtering and masking procedures to enhance the true land/water interface and eliminate artefacts, the coastline is vectorized. A quantitative comparison of the simulated coastlines and the ones derived from the remotely sensed images is reported by Milne (2003).

Figure 8 shows the derived coastlines for an image near low tide on 13 September 1999. Visually, there is good overall agreement between the modelled and retrieved land/water interface in the western part of the image but the accuracy degrades east of Grand-Pré (see Fig. 2 for locations). Milne (2003) reports that the mean separation between the two coastlines is 141 m, with 14% of the points within 25 m and 37% within 100 m. An important source of discrepancy is the local bathymetry. The abrupt reduction in data density east of $64^{\circ}18'W$ longitude (Fig. 2) and lack of data in the channels between the mainland and Boot Island leads to the model underpredicting the shoreward extent of the land/water interface in this area.

A comparison of the derived coastlines at high tide (Fig. 9) shows that the model over-predicts the inundation of large areas along the river beds on the eastern half of the area and there is extensive flooding of the Grand-Pré area in the centre of the image. These areas are extensively dyked and the

flooding appears to be due to the fact that the dykes, although in the original topographical data, are not resolved in the model (with 30 m) resolution.

5 Error assessment

Figure 10 shows the sea level error (Section 3b) at the Minas Basin Station for the simulations with no correction and with Correction 1. Spectral analysis confirms that the remaining error is dominated by the semidiurnal tides (Fig. 11). The fact that the semidiurnal error is an order of magnitude larger than the other errors indicates that further improvements in the tidal modelling are required to reduce further the error in the instantaneous water level.

The diurnal tidal errors are slightly reduced by Correction 1 (Fig. 11) and further reduced by Correction 2 (not shown). There is, however, a large increase in the error associated with the M_4 tide (period near 6 h). The M_4 component is not part of the tidal boundary conditions and the correction method is projecting the M_4 from the Saint John record back onto the boundary. The fact that this increases the error suggests that M_4 and other high frequency tides should be removed from the Saint John record prior to the correction process. An additional run was performed to verify this statement. The energy close to the 6-hour period was removed



Fig. 9 True colour Landsat-7 image of the Wolfville vicinity at 14:52:00 (GMT) on 13 July 2000. The image was taken near high tide. The red line is the instantaneous coastline extracted from one of the near infra-red bands and the blue line is the coastline extracted from the tidal model. The analysis is reported in Milne (2003). Image courtesy of Trevor Milne and the Applied Geomatics Research Group.

from the correction prior to the run (in all other respects the same as the run with Correction 2). The 6-hour period spectral peak in the error was reduced to the level observed with no correction (not shown). The other spectral peaks remained unchanged. In terms of the r.m.s. error, this translates into a further 2-cm improvement.

Confidence limits were estimated for the spectral estimates in Fig. 11 using standard MATLAB routines. The only significant changes at the 95% confidence level are the improvement in the semidiurnal constituents and the degradation of the M_4 .

The origin of the spectral peak between the M_2 and the M_4 , at 8.2 hours, is not clear. There are no tri-diurnal constituents with significant amplitude. A possible explanation is the natural resonance of the Bay of Fundy (excluding the Gulf of Maine) which was estimated at nine hours by Rao (1968). The spectral peaks near four and three hours are M_6 and M_8 respectively.

Since the errors in the semidiurnal constituents dominate the overall error, we searched for a systematic bias that might be corrected. Figure 12 shows the relative amplitude error and phase error as a function of the observed amplitude for the three semidiurnal constituents. The fact that the M_2 phase and relative amplitude errors are independent of amplitude, a proxy for along-channel position, suggests that corrections to

the amplitude and phase at the boundary are called for. The relative amplitude errors for N_2 tend to increase with amplitude and the errors for S_2 do not have a pattern. The bias towards positive amplitude errors for M_2 and N_2 means that the model underestimates the tidal amplitudes. This, plus the fact that the relative errors are small at Saint John, suggests that there is too much friction in the model.

We performed two experiments with the five-constituent model in which we slightly altered M_2 and N_2 at the open boundary based on the biases shown in Fig. 12. The alteration for M_2 was a uniform increase of 0.05 m in the amplitude and a phase decrease of 2° . For N_2 , the phase was decreased by 10° and the amplitude was not changed. Modification of M_2 alone leads to a 0.04 m improvement in the error metric for M_2 and 0.03 m for N_2 . Modification of both M_2 and N_2 leads to no improvement in M_2 and a 0.09-m improvement in N_2 . These results highlight the complex dynamical interactions between M_2 and N_2 . The likely reason for the interactions relates to the near resonance of N_2 and the likelihood that its amplitude is limited by the damping from M_2 (Ku et al., 1985; Garrett, 1972). As a result, small changes in the overall dissipation change the resonance behaviour of both M_2 and N_2 . The S_2 constituent, which is further from resonance than M_2 and N_2 , does not exhibit the same sensitivity. Other mechanisms for

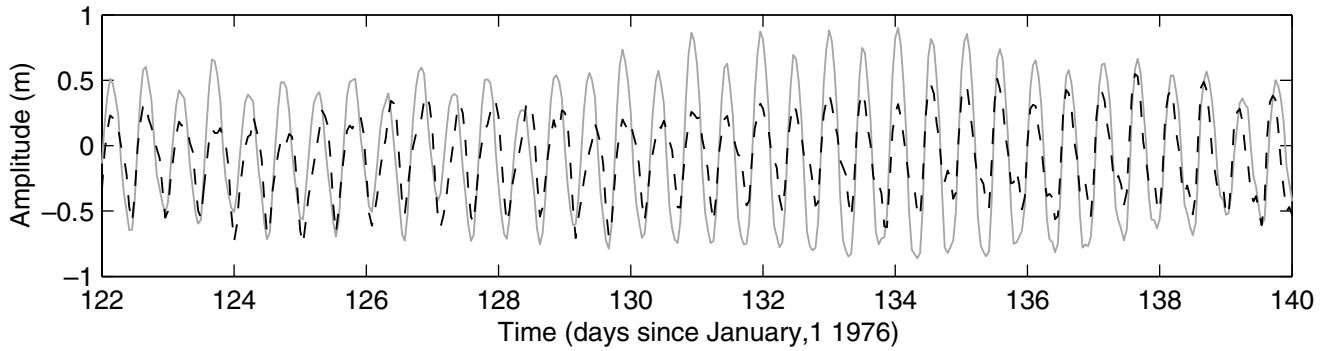


Fig. 10 Elevation residual at Minas Basin Station as a function of time for no correction (solid grey line) and Correction 1 (dashed black line).

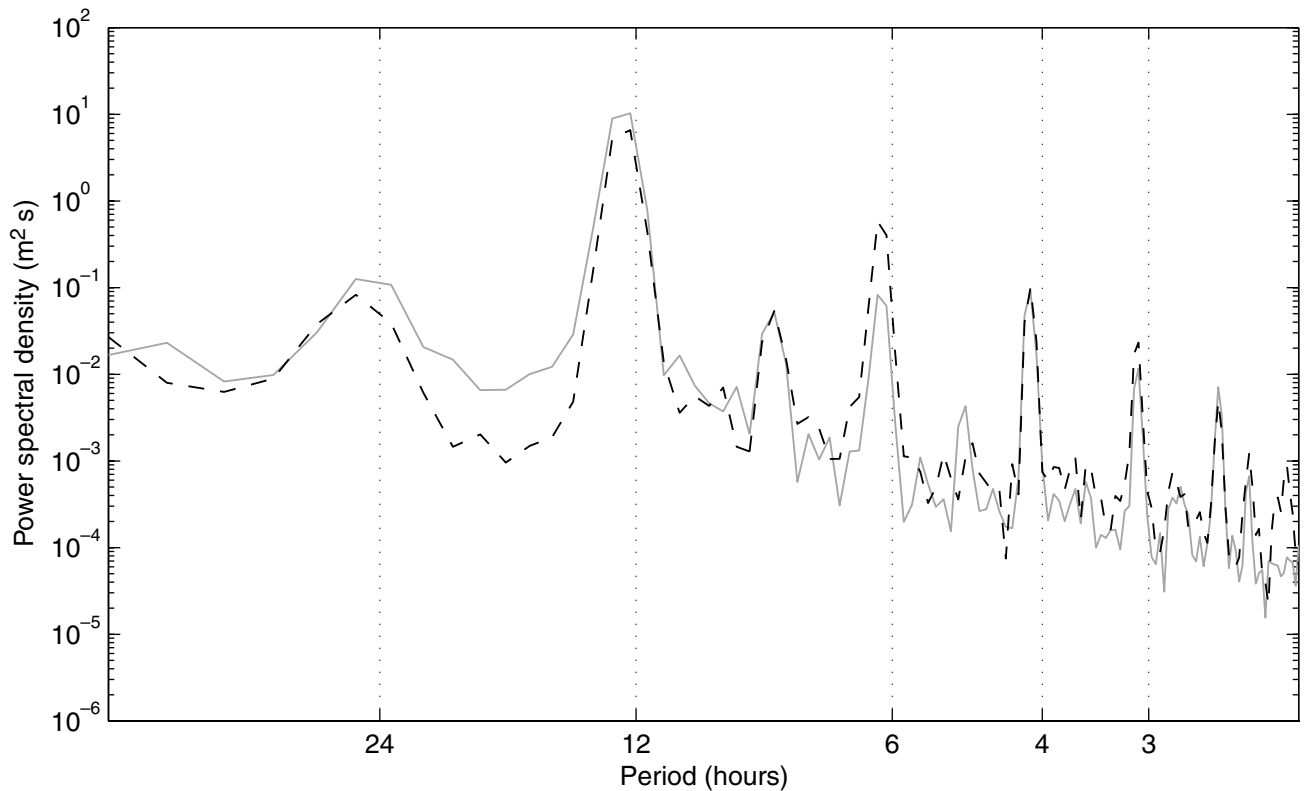


Fig. 11 Power spectrum of the elevation residual for no correction (solid grey line) and Correction 1 (dashed black line) at Minas Basin Station.

non-linear interaction between M_2 and N_2 include the advection of momentum and the non-linearity in the continuity equation (due to the fact that the surface displacements are a significant fraction of the depth).

The sensitivity of the model to the value of the bottom friction coefficient, C_d , was investigated by performing two runs using the five-constituent model in which M_2 was corrected for its observed bias as previously. Table 6 shows the effect of decreasing the friction parameter on the elevation error per constituent. M_2 tends to degrade while N_2 improves. The improvement was not sufficient, however, to push the N_2 error below the value obtained using the solution of the assimilation system for

the Northwest Atlantic (Dupont et al., 2002). The other constituents are not very sensitive to changes in C_d .

6 Discussion

The results show that the modelling system is capable of accurate simulation of the water level in the Bay of Fundy with r.m.s. errors in Minas Basin on the order of 0.3–0.5 m or 10%. The primary improvement was in the simulation of the M_2 tide in Minas Basin where the phase errors and relative amplitude errors were reduced to levels similar to the rest of the Bay of Fundy. This represents an important advance as the M_2 solution in Minas Basin has been a weakness in previous modelling

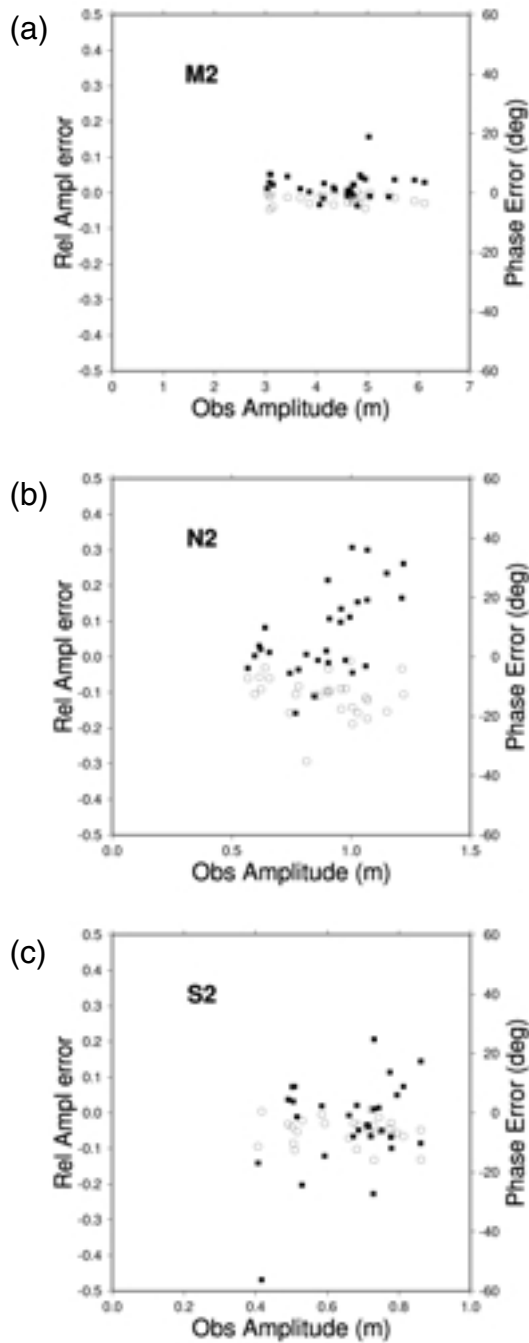


Fig. 12 Relative amplitude error (solid squares) and phase error (open circles) as a function of the observed amplitude of the given constituent. The amplitude serves as a proxy for the distance up the bay.

efforts. We believe that the new bathymetry data in Minas Channel, which connects the basin to the rest of the bay, was an important contributor to the improved solutions.

When considering how to reduce the model errors further, several properties of the solutions need to be considered. Firstly, the errors in the simulation of the sea level in Minas Basin are still dominated by the semidiurnal tides. Secondly, the errors in M_2 and N_2 , while relatively small, are significant

relative to the 95% confidence limits on the observations. Thirdly, the phase errors and the amplitude errors make roughly equal contributions to the overall error.

Overall these solutions have a bias in that the M_2 and N_2 amplitudes are too small and the phases late. Two possible explanations are: the open boundary conditions need to be adjusted or there is too much friction in the system. In Section 5 we showed that decreasing the drag coefficient improved N_2 and degraded M_2 . We also showed that adjusting the M_2 boundary conditions to correct for the almost constant phase and relative amplitude errors improved both M_2 and N_2 . An additional correction to the N_2 phase resulted in further improvements in N_2 , however, the gain in M_2 was lost. It is also possible that small increases in water depth in Minas Channel could be used to reduce the bias.

A feature of the N_2 errors is that the relative amplitude error increases towards the head of the bay. This is in contrast to M_2 where the relative amplitude error is roughly constant over the bay. We interpret this to mean that the near-resonant amplification of N_2 is being overdamped. However, trying to decrease the dissipation by reducing the drag coefficient causes the M_2 solution to degrade. This is an example of the tight coupling between the M_2 and N_2 tidal harmonics (Section 5) that will complicate attempts to improve the simulations.

There are several potential sources of error related to bottom friction. For example, the order of magnitude variations in the dissipation in Minas Channel and Basin (Fig. 7) suggest different erosion regimes that might lead to spatial variations in bottom roughness and drag coefficient. Also, the present model is vertically integrated and there may be errors in the dissipation due to the lack of vertical structure. Given that the remaining errors in amplitude and phase are small and the importance of the dissipation in the overall behaviour of M_2 and N_2 , accounting for the vertical structure and spatial variations may play a role in future improvements.

Another issue is baroclinic effects. Recent observations of large amplitude internal tides in the deep basin at the mouth of the Bay of Fundy (Alex Hay, personal communication 2003) raises the possibility that baroclinic processes might affect the tides through extraction of energy from the surface tide and through modification of the bottom friction. It also raises the possibility of seasonal modification of the tidal constituents through changes in dissipation, especially M_2 and N_2 which are sensitive to the overall dissipation in the system.

A potential source of systematic error in the observations is the 18.6-year nodal modulation. Ku et al. (1985) showed that for the M_2 tide, frictional effects reduced the modulation to 2.5% from the astronomical value of 3.73%. The nodal modulation factor is a standard feature of tidal analysis and synthesis as it allows for the calculation of tidal constituents that are independent of the 18.6-year nodal modulation. However, in the Bay of Fundy, the astronomical value leads to potential systematic errors of about 1%, which becomes an important component of the error budget when trying to drive the simulation errors below 10%. In addition, the modulation of the tidal constituents over the lunar perigean cycle (Godin, 1988) may contribute a systematic error.

Other potential contributions to the error budget are the changes in the Bay of Fundy tides during the period of the systematic collection of tidal data. Godin (1992) estimates that the M_2 tide at Saint John is increasing by about 0.07 m per century. This suggests an increase in Minas Basin of about 0.1–0.2 m per century. These changes in M_2 tidal amplitude are a result of the regional subsidence and the consequent changes in the resonant system due to increased water depths. The collection of the tide gauge data was concentrated in the 1960s and 1970s. Thus, an analysis that combines data from the 1960s with that from the current decade introduces an uncertainty in M_2 of about 0.04–0.08 m. The use of the TOPEX/Poseidon data in the assimilation scheme is not expected to be a large problem because changes in the Gulf of Maine are expected to be small. However, it may make a small contribution to the error budget. In the future, the projected changes in the M_2 tide have the potential to make a significant contribution towards the total error.

The comparison between the land/water interface in the model and that derived from remotely sensed observations highlights the fact that good simulation of the sea level is a necessary but not sufficient condition for accurate simulation of the instantaneous coastline. Simulating the coastline requires good representation of channels, which provide flooding pathways as described in relation to the under-prediction of inundation near Boot Island in Fig. 8, and of linear features such as dykes, which prevent flooding of low areas as described in relation to the excessive inundation along river banks and around Grand-Pré in Fig. 9. Other important issues are: the fact that the bathymetry (depth below mean sea level) is less well known than the topography (height above mean sea level); the fact that the two datasets are often not referenced to the same vertical datum; and that different datasets often use different geoids (e.g., NAD27 versus NAD83).

One way to handle long narrow features such as dykes is to incorporate specialized dyke elements as implemented by Westernink and Luettich in their model for the flooding of New Orleans (Rick Luettich, personal communication, 2003). Another possibility is to discontinue modelling the details of the inundation with a dynamical model. Geographical Information System (GIS) technology exists to use the instantaneous water level near the coast to flood a detailed digital elevation model (DEM) with much higher spatial resolution than can be done dynamically. This has been done for flood risk assessment for Charlottetown PEI (O'Reilly et al., 2003) and Truro NS (O'Reilly et al., 2002). Milne (2003) flooded a high resolution (2 m) DEM of the Cornwallis River and found that using the DEM reduced the mean separation between the derived coastlines from 56 m to 35 m and increased the percentage of points with a separation of less than 25 m from 44% to 67%.

There are at present no estimates of the accuracy of the instantaneous coastline derived from remotely sensed data. The goal of this work was to provide estimates of the sea level that could be used to estimate coastlines for comparison in two ways: 1) through extraction of the instantaneous coastline from the model; and 2) to flood available DEMs. The preliminary analysis reported in Milne (2003) is encouraging.

However, we can use the model error to estimate a lower bound on the expected agreement between the tidal model and remotely sensed data. The r.m.s. error in the sea level estimate is 0.5 m. Given a beach slope of 1% this results in a horizontal error of 50 m. The error will be larger for more gentle slopes and smaller for steeper slopes.

7 Conclusions

The modelling system presented here is capable of accurate simulation of the water level in the Bay of Fundy. The r.m.s. error for the M_2 tidal harmonic is less than 0.3 m (relative to a tidal amplitude of 3 m at Saint John and over 5–6 m in Minas Basin). The system can also simulate the series of total water level in Minas Basin with an r.m.s. error of 0.3–0.5 m, relative to an r.m.s. signal of 3.6 to 4.5 m. Overall, the system is capable of an accuracy of ~10% in Minas Basin.

The system is suitable for a model-based tidal prediction system and for the tidal component of an operational water level (storm surge) prediction system for the Bay of Fundy. As well, a system for sediment transport and erosion studies could be created with the addition of a sediment transport module.

The tight coupling between the M_2 and N_2 tidal harmonics will complicate attempts to improve the simulations. A systematic approach will have to consider the joint response of M_2 and N_2 to the following: 1) changes in tidal boundary conditions, including their cross-channel structure; 2) the magnitude and spatial structure of the drag coefficient; and 3) small changes in water depth. In addition, the vertical structure of the currents and the baroclinic tide at the mouth of the bay may require consideration in order to improve the model accuracy.

The comparison of the land/water interface from the model and remotely sensed data shows that accurate simulation requires both a good simulation of the sea level and accurate representation of the topography, especially features such as channels and dykes that have a major influence on the horizontal position of the land/water interface. The analysis report here and visual examination of the images in Milne (2003) supports the hypothesis that the image analysis techniques provide a reasonable estimate of the instantaneous coastline.

Acknowledgements

This project was funded by the Earth and Environment Applications Program of the Canadian Space Agency with additional support from the CHS. We thank John Loder for his vision and leadership in getting the terrestrial and ocean scientists to meet on the beach. We thank Tim Webster, Robert Maher, Daniel Deneau, and Trevor Milne of the Applied Geomatics Research Group at the Centre of Geographic Sciences for their active participation in the project. Trevor Milne provided us with the analysis and images in Figs 8 and 9. We thank John Hughes Clarke (University of New Brunswick) and the Geological Survey of Canada (Atlantic) for the high resolution bathymetry data in Minas Channel. We also thank Charlie O'Reilly (CHS) for the tidal constituent database and Jason Chaffey for help manipulating the database.

References

- BAY OF FUNDY TIDAL POWER REVIEW BOARD (CANADA). 1977. Reassessment of Fundy tidal power. Report prepared for the Minister of Supply and Services (Canada), under contract No. 02KX 23384-5207. 516 pp.
- CARRÉRE, L. and F. LYARD. 2003. Modeling the barotropic response of the global ocean to atmospheric wind and pressure forcing - comparisons with observations. *Geophys. Res. Lett.* **30**: 1275.
- DÉNEAU, D. 2002. Extracting 3D coastlines from remotely sensed data. Project report for the Department of Fisheries and Oceans (DFO) and the Canadian Space Agency (CSA). Available from Tim Webster, Applied Geomatics Research Group, Centre of Geographic Sciences, Middleton, N.S., Canada. 71 pp.
- DEWOLFE, D.L. 1977. Tidal measurement program of the Bay of Fundy–Gulf of Maine tidal regime. *Lighthouse*, **15**: 17–24.
- . 1986. An update on the effects of tidal power development on the tidal regime of the Bay of Fundy and Gulf of Maine. In: *Effects of changes in sea level and tidal range on the Gulf of Maine-Bay of Fundy system*, G.R. Daborn (Ed.), Acadia Centre for Estuarine Research, Wolfville, NS, Canada, pp. 35–54.
- DROZDOWSKI, A.; C. HANNAH and J. LODER. 2002. The northwest Atlantic tidal current database. *Can. Tech. Rep. Hydrogr. Ocean Sci.* **222**:v+35pp. Available online from the DFO library at <http://www.dfo-mpo.gc.ca/Library/265853.pdf>.
- DUPONT, F.; C.G. HANNAH, D.A. GREENBERG, J.Y. CHERNIAWSKY and C.E. NAIMIE. 2002. Modelling system for tides for the North–west Atlantic coastal ocean. *Can. Tech. Rep. Hydrogr. Ocean Sci.* **221**:vii+72pp. Available online from the DFO library at <http://www.dfo-mpo.gc.ca/Library/265855.pdf>.
- GARRETT, C. 1972. Tidal resonance in the Bay of Fundy and Gulf of Maine. *Nature*, **238**: 441–443.
- . 1974. Normal resonance in the Bay of Fundy and Gulf of Maine. *Can. J. Earth Sci.* **4**: 549–556.
- GODIN, G. 1988. The resonant period of the Bay of Fundy. *Cont. Shelf Res.*, **8**: 1005–1010.
- . 1992. Possibility of rapid changes in the tides in the Bay of Fundy, based on a scrutiny of the records from Saint John. *Cont. Shelf Res.* **12**: 327–338.
- GREENBERG, D.A. 1979. A numerical model investigation of tidal phenomena in the Bay of Fundy and Gulf of Maine. *Marine Geodesy*, **2**: 161–187.
- ; F.E. WERNER and D.R. LYNCH. 1998. A diagnostic finite-element ocean circulation model in spherical-polar coordinates. *J. Atmos. Ocean Tech.* **15**: 942–958.
- ; J.A. SHORE, F.H. PAGE and M. DOWD. 2005. Modelling embayments with drying intertidal areas for application to the Quoddy region of the Bay of Fundy. *Ocean Modelling*, (Special Issue on the International Workshop on unstructured grid numerical modelling of coastal, shelf and ocean flows, Delft Sept. 2003), in press.
- KU, L.-F.; D.A. GREENBERG, C.J.R. GARRETT and F.W. DOBSON. 1985. Nodal modulation of the lunar semidiurnal tide in the Bay of Fundy and Gulf of Maine. *Science*, **230**: 69–71.
- LYNCH, D. AND F. WERNER. 1991. 3-D hydrodynamics in finite elements. Part II: Non-linear time-stepping model. *Int. J. Num. Methods Fluids*, **12**: 507–533.
- ; J.T.C. IP, C. E. NAIMIE and F.E. WERNER. 1996. Comprehensive coastal circulation model with application to the Gulf of Maine. *Continental Shelf Res.* **16**: 875–906.
- ; C.E. NAIMIE and C.G. HANNAH 1998. Hindcasting the Georges Bank circulation, Part I: Detiding. *Continental Shelf Res.* **18**: 607–639.
- MILNE, T. 2003. Tide model validation using remotely sensed data: Minas Basin N.S. Report available from Tim Webster, Applied Geomatics Research Group, Centre of Geographic Sciences, Middleton, N.S., Canada, 68 pp.
- O'REILLY, C.; H. VARMA and G. KING. 2002. The 3-D coastline of the new millennium: managing datums in N-dimension space. In: *Vertical Reference Systems*, International Association of Geodesy Symposia, H. Drewes, A.H. Dodson, L.P.S. Fortes, L. Sanchez and P. Sandoval (Eds), Springer-Verlag, Berlin, Germany, Vol. 124, pp. 276–281.
- ; D. FORBES and G. PARKES. 2003. Mitigation of coastal hazards: Adaptation to rising sea levels, storm surges and shoreline erosion. *CDROM Proceedings, 2003 Annual Conference, Canadian Society for Civil Engineering*, Moncton, 4–7 June 2003, P. 257, CSN410 pp. 1–10.
- PAWLOWICZ, R.; B. BEARDSLEY and S. LENTZ. 2002. Classical tidal harmonic analysis including error estimates in MATLAB using T_TIDE. *Computers Geosci.* **28**: 929–937.
- RAO, D.B. 1968. Natural oscillations of the Bay of Fundy. *J. Fish. Res. Bd., Canada*, **25**: 1097–1114.
- SANKARANARAYANAN, S. and D.F. MCCAY. 2003. Three-dimensional modeling of tidal circulation in the Bay of Fundy. *J. Waterway, Port, Coastal, Oc. Eng.* **129**: 114–123.
- SMAGORINSKY, J. 1963. General circulation experiments with the primitive equations I: the basic experiment. *Mon. Weather Rev.* **91**: 99–164.

